Proceedings of the 1991 IEEE International Symposium
on Intelligent Control
13 - 15 August 1991, Arlington, Virginia, U.S.A.

DISPLACEMENTS THAT NULL FORCES

M. Griffis, C. Crane, & J. Duffy
Center for Intelligent Machines and Robotics
University of Florida
Gainesville, FL 32611

Abstract

Experimental results indicate that the inner product defined by stiffness does in fact provide the correct force-error nulling directions along which to move a robotic end-effector. These directions, which are defined as the "twists of compliance," form the [K]-orthogonal complement to the twists of freedom of a partially constrained gripper (where the matrix [K] describes the stiffness of the robot and not its task). This implementation of kinestatic control is accomplished via the synthesis of two scalar gains to effect the six-dimensional, simultaneous control of force and displacement.

1 Introduction

This paper documents the six-dimensional implementation of the theory of kinestatic control [1] on a robot system comprising a modified General Electric P60 robot, two 386PC computers, three Creonics motion controller cards, a Lord ATI Corp. model 15/50 force/torque sensor, and a homemade un-instrumented compliant device. (See Figure 1.) Essentially, one of the computers (ROBOT) was employed to control the fine-position displacement of the end-effector of the robot, while the other (KINESTATIC) was employed to generate the twist commands of the end-effector platform. (Communications between the two asynchronously operating PCs was over Ethernet and consisted of an end-effector platform twist command sent one way and an actual position and orientation of the end-effector sent the other.) The end result of this assemblage of hardware and software provided a convenient test-bed upon which to verify the theory.

A liberal amount of compliance was introduced into the end-effector of the robot by the compliant device.[1] Figure 1 illustrates this and the force/torque sensor that constitutes the last link of the robot. The arrangement – robot-force/torque sensor-compliant device-gripper – can be simplified conceptually, without a loss of generality, in order to explain the objective of this work, viz. to properly use displacements to control forces.

Consider the planar two-dimensional example illustrated in Figure 2. A wheel is connected to a platform via two translational springs, which are capable of compression as well as tension. The platform is then subsequently connected to ground via two actuated prismatic (slider) joints that are tuned for fine-position control. The wheel is to maintain contact with a rigid environment. The center point of the wheel thus has a single freedom, which is a displacement p_t in the direction of $\vec{u}_t$. Based on the constraint imposed upon the wheel, a normal contact force, f_n acting through the center point along $\vec{u}_n$, may interact between the wheel and the environment.

The control of f_n along $\vec{u}_n$ and p_t along $\vec{u}_t$ is accomplished by judicious choices of slider displacements δd_1 and δd_2, which together combine to move the platform in some direction. Intuitively, one may at the outset consider that the *best* motion for nulling errors in the force f_n would be a displacement of the platform in the $\vec{u}_n$ direction, i. e. parallel to the normal force. However, this is not the case, and in general, the best displacement is in some other direction, $\vec{u}_c$, which is canted to $\vec{u}_t$ at an angle not necessarily equal to 90°. *The best displacement is one that changes the force error in a desired way without affecting the control of the wheel's displacement in the $\vec{u}_t$ direction.* For example, displacing the platform in the $\vec{u}_c$ direction would not move an at-rest wheel, but it would change the normal force.

For this simple example, a positive-definite Euclidean inner product mandates that a displacement along $\vec{u}_n = \cos(\theta_n)\,\vec{i} + \sin(\theta_n)\,\vec{j}$ is Euclidean-orthogonal to a displacement along $\vec{u}_t = \cos(\theta_t)\,\vec{i} + \sin(\theta_t)\,\vec{j}$. In other words,

$$\vec{u}_t^{\,T}\,\vec{u}_n = 0. \tag{1}$$

However, these vectors are elements of a Euclidean vector space, which uses two *non*-homogeneous coordinates to locate ∞^2 elements.[2] (See Ryan [8].) Even though there exists a purely geometrical positive-definite inner product here in this simple case, it is not the best one with which to perform twist decomposition.

It is proposed here that stiffness can be used to define a proper inner product with which to obtain the *best* f_n-error-nulling direction: $\vec{u}_c = \cos(\theta_c)\,\vec{i} + \sin(\theta_c)\,\vec{j}$. In other words, for coordinates $\vec{u}_t = [\cos(\theta_t), \sin(\theta_t)]^T$ and $\vec{u}_c = [\cos(\theta_c), \sin(\theta_c)]^T$,

$$\vec{u}_t^{\,T}\,[K]\,\vec{u}_c = 0, \tag{2}$$

where the 2x2 matrix [K] is symmetric, and its three elements have the dimension F/L. (Eq. (2) establishes that the two displacement directions are "[K]-orthogonal.") The matrix [K] quantifies the stiffness of the mechanism consisting of a wheel connected to ground by two translational springs, a platform, and two actuated sliders. (It does not quantify its task, which is the surface to be tracked by the wheel). It is assumed that the actuated sliders are stiff (they are tuned for fine-position control), and since they act in series with the more compliant translational springs, their compliances can be neglected, and the stiffness of the overall mechanism is thus solely due to the translational springs.

In general, the stiffness matrix in (2) establishes a mapping of stiffness that transforms a small displacement ($\delta\vec{d}$) of the center point of the wheel into a small change in normal force ($\delta\vec{f}$) which acts through the center point of the wheel:

[1] Other researchers have introduced compliance into their end-effectors (see for example [2] – [6].), but the authors consider that none have used the knowledge of actual compliance to establish the proper directions in which to move to control force.

[2] A Euclidean vector space does not possess the power of locating infinite elements with finite coordinates. Once a rotational coordinate is incorporated with the two translational ones (general planar rigid body motion), then a rotation about a point at infinity yields a pure translation, and accordingly, three finite homogeneous coordinates are used to describe general planar motion. Because the resulting homogeneous twist coordinates would no longer belong to a Euclidean vector space, a positive-definite inner product acting on them must be non-Euclidean. (See [7], for the non-Euclidean geometry of stiffness.)

CH3019-7/91/0000-0110$01.00 ©1991 IEEE

$$\delta\vec{f} = [K]\,\delta\vec{d}. \quad (3)$$

Consider a numerical example of $\theta_1 = 45°$, $\theta_2 = 90°$, and $k_1 = k_2 = 10$ kg/cm. (It is assumed that the two springs do not deviate too far from their respective free lengths.) Then, the stiffness matrix in (2) and (3) assumes the form,

$$[K] = \begin{bmatrix} 5. & 5. \\ 5. & 15. \end{bmatrix} \text{kg/cm}.$$

The stiffness matrix [K] is not dependent on the task required of the wheel. (It is not dependent on either θ_n or θ_t.) The direction $\vec{u}_c$ is encountered when investigating which displacement direction is related to a change in force in the $\vec{u}_n$ direction. In other words, from (3),

$$\lambda\,\vec{u}_n = [K]\,\vec{u}_c, \quad (4)$$

where λ is a non-zero magnifying scalar (dimension F/L). Dividing (4) by λ and substiting for $\vec{u}_n$ in (1) establishes (2) as the proper condition for $\vec{u}_c$ to be best direction to displace the platform to control the normal force in the $\vec{u}_n$ direction. *For the numerical example,* $\theta_t = 135°$, and therefore, from (2) with the above [K], $\theta_c = 180°$. Therefore, in this work, a task-independent mapping of stiffness, [K], defines the inner product that separates a freedom direction from a compliance direction (Eq. (2)).

The control of the normal force is accomplished without displacing the wheel by displacing the platform in the $\vec{u}_c$ direction. (The force-error correcting displacement is $\delta\vec{d}_c = \delta p_c\,\vec{u}_c$, where δp_c has dimension L and quantifies a small displacement in the $\vec{u}_c$ direction.) It is important to recognize this since now, by superposition, a desired allowable displacement of the wheel,

$$\delta\vec{d}_t = \delta p_t\,\vec{u}_t, \quad (5)$$

can be accomplished by simply adding it to the force-error correcting displacement, $\delta\vec{d}_c$. (Because $\delta\vec{d}_t$ is an allowable displacement, adding it to $\delta\vec{d}_c$ does not affect the control of normal force.) Therefore, the following small slider displacements can be computed to control the normal force and the tangential displacement simultaneously:

$$\delta\vec{d} = G_t\,\delta p_t\,\vec{u}_t + G_c\,(\delta f_n/\lambda)\,\vec{u}_c, \quad (6)$$

where $\delta\vec{d} = [\delta d_1, \delta d_2]^T$ establish the slider displacements. Now, for the numerical example given in the paper, $\vec{u}_t = [-0.707, 0.707]^T$, $\vec{u}_c = [-1., 0]^T$, and $1/\lambda = 0.1414$ cm/kg. In (6), G_t and G_c are dimensionless scalar gains, and δp_t and δf_n are errors in wheel position and normal force. Successive applications of (6) based on updated errors in δp_t and δf_n provides the means for controlling both the tangential wheel position and the normal force.

The experimental work detailed in this paper is essentially a six-dimensional experimental extension of the slider actuators-platform-springs-wheel arrangement shown in Figure 2. Therefore, with the force/torque sensor constituting the "platform" that was connected to ground by six non-back-drivable actuators, it remained to twist it relative to ground (with six degrees-of-freedom) in order to simultaneously control the constraint wrenches and twist freedoms of the gripper. For the implementation, the "gripper" was a three inch long bar of aluminum square stock, drilled and tapped. (See Figure 1 which shows the gripper bolted to a large immovable table.)

2 Empirical Determination of [K]

Prior to simultaneously controlling force and displacement, it was necessary to first measure the mapping of stiffness for the robot, which establishes the relationship given by

$$\hat{w} = [K]\,\hat{D}, \quad (7)$$

where the six wrench increment coordinates are $\hat{w} = [\delta\vec{f};\ \delta\vec{m}_O]$ and the six twist coordinates are $\hat{D} = [\delta\vec{x}_O;\ \delta\vec{\phi}]$. (A wrench increment is a change in the resultant of the forces and torques that are externally applied to the gripper, and a twist is a small change in position/orientation of the gripper relative to the force/torque sensor.) This relationship was empirically measured while the robot was in the configuration shown in Figure 1, where the gripper was bolted to the table. During the measurement the force/torque sensor was used to record the data on the forces/torques (wrenches) applied to the end-effector by the table. The six actuator encoders were used, and their sum total effect was representative of the twist of the force/torque sensor relative to ground, and hence of the grounded gripper relative to the force/torque sensor. From (7), it was clear that a minimum of six of these twists were necessary to measure [K], provided they were independent. Because the compliance of the servoing robot was considered very low compared to that of the compliant device connected in series, the deflections of the robot were not measured during the determination of [K]. The four factors that were considered to have influenced the measurement of robot stiffness are given by the following:

i) force/torque sensor (wrench measurement) resolution,
ii) encoder (twist measurement) resolution,
iii) linearity, and
iv) robot configuration.

Not only was the resolution in the individual coordinates considered, (f_x for instance was 0.02 kg, and m_{ox} was 0.02 kg-cm), but it was also necessary to consider the resolution in obtaining direction and location information from the measured wrench and twist coordinates. Therefore, one must displace the robot (command it to move) significantly enough to obtain a measurable (and more accurate) $\hat{D}$, viz. it is necessary to accurately locate the twist together with its direction, pitch, and magnitude. This commanded twist must provide, through a reasonable amount of compliance, an accurate measure of wrench increment ($\hat{w}$), viz. an accurate determination of its location, direction, pitch, and magnitude.

It is important to note that the robot was not given too large a displacement (twist) for which the matrix [K] would lose its linearity. Such a set of six independent large twists taken together with their corresponding six wrench increments would yield a matrix [K] that would not map correctly a linear combination of the original six twists.

In order to convince the investigator that the compliance of the robot was negligible, the robot configuration was changed, and measurements for [K] were repeated. A stiffness matrix [K] for each of two different robot configurations is presented here.

Initially, a Remote Center-of-Compliance (Lord ATI Corp. RCC) device was installed. However, this device was too stiff for axial displacements and cocking rotations.[3] In other words, because the force/torque sensor tended to saturate, the robot could not be displaced far enough in these directions to obtain an accurate and repeatable measure of $\hat{D}$. A second effort resulted in a spatial spring that was far too compliant, which meant that sufficient forces/torques could not be applied to the spring. A third and final assemblage (three compression springs each clamped at both ends) is shown in Figure 1. This yielded the repeatable and

[3]The RCC was not designed for force control, but rather it was designed to avoid it.

manageable stiffness matrix:

$$[K] = \begin{bmatrix} 3.140 & -0.168 & -0.344 & -1.051 & 34.898 & -0.083 \\ 0.197 & 3.439 & 0.052 & -31.914 & -0.783 & 0.057 \\ -0.295 & 0.366 & 11.194 & 5.049 & -1.159 & -0.093 \\ -1.381 & -28.511 & -2.082 & 394.018 & -5.979 & 2.235 \\ 25.660 & -1.342 & -2.008 & 2.243 & 377.047 & 5.944 \\ 0.959 & 0.087 & 0.073 & -8.484 & 8.377 & 76.698 \end{bmatrix}.$$

The upper-left 3x3 has units of kg/cm, the lower-right 3x3 has units of kg-cm, and the other two 3x3s have units of kg. It should be noted that [K] is asymmetric and that its symmetric part $([K] + [K]^T)/2$ is positive-definite. That the symmetric part is positive-definite is a necessary condition for the general control of force. (See Griffis [7].)

The coordinate system used to express [K] was located at the center of the force/torque sensor. The z-axis was coaxial with the sixth joint of the robot, and the x-axis defined the reference for the last joint of the robot. (This coordinate system is referenced by the label **F**.) This choice of representation proved to be the most convenient, but another one could have just as well been used to establish a different representation, [K′], where $[K'] = [E]^T[K][E]$, and the 6x6 matrix [E] represents the transformation of twist coordinates. (In other words, the same twist needs a pair of twist coordinates $\hat{D}$ and $\hat{D}'$, one set for each coordinate system. Then, $\hat{D} = [E]\,\hat{D}'$.)

While the gripper was grounded and the compliant device was in an unloaded configuration, the matrix [K] was measured by sequentially moving the six individual actuators of the robot, and recording the changes in the forces and torques (wrench increment) applied to the end-effector. In other words, the six independent twists chosen were the individual actuator displacements themselves. (This choice ensured the directions and locations of the respective twists, while at the same time it enabled easy monitoring of twist magnitude.) Twists were referenced so to describe the gripper's motion relative to the platform (force/torque sensor). The following steps were taken to find [K] in terms of **F**:

i) While holding the last five actuators fixed, the first actuator was moved 133 encoder edges, which corresponded to 0.25° degrees of the first joint. The twist and wrench increment were expressed in terms of **F** and recorded. The actuator was then returned to its original location, and the same command was given again. This process was performed ten times. The sum of the twist data was stored in $\hat{D}_1$, and the sum of the wrench data was stored in $\hat{w}_1$.

ii) Step (i) was repeated for joints 2 through 6 in turn, and this generated the twist data $\hat{D}_i$ and wrench data $\hat{w}_i$, (i = 2, ..., 6). The following summarizes the displacements commanded to the actuators:

Actuator	Command	Corresponding Joint Command
1	133 4X encoder edges	0.25°
2	230	0.25
3	139	0.15
4	277	0.5
5	185	0.5
6	150	0.5

iii) The wrench data, $\hat{w}_1$, ..., $\hat{w}_6$ was assembled as columns in a 6x6 matrix [W], and the twist data, $\hat{D}_1$, ..., $\hat{D}_6$ was likewise assembled as the columns of a 6x6 matrix [D]. From (7), these matrices are related [W] = [K] [D], and therefore [K] was determined by inverting [D].

iv) In order to check for linearity, twists that were not used to determine [K] were commanded, and the actual measured wrench increments were compared to those computed using [K]. The twists commanded were in fact the six cardinal twists of **F**. The end-effector (force/torque sensor) was successively given small displacements in the x, y, and z directions, and then successive small rotations about the x, y, and z axes. These twists effected six wrench increments that corresponded respectively to scalar multiples of the six columns of [K].

v) In order to investigate the dependence of robot configuration on [K], the last joint was rotated 90°, and steps (i) – (iii) were repeated.

This represented a significant change in the robot configuration as seen from the force/torque sensor and spatial spring, since the first five joints all moved relative to them. A stiffness matrix that was measured in the second robot configuration was

$$[K] = \begin{bmatrix} 3.708 & -0.175 & -0.282 & -0.653 & 28.950 & 0.000 \\ 0.094 & 3.167 & -0.190 & -35.810 & 3.678 & -0.129 \\ -0.310 & -0.095 & 11.298 & -2.568 & 4.686 & -0.001 \\ -1.841 & -26.456 & -0.373 & 385.484 & -2.320 & 8.246 \\ 30.373 & -1.016 & -0.751 & -2.486 & 352.869 & 9.167 \\ 0.791 & 0.181 & 0.046 & -0.949 & 13.464 & 76.315 \end{bmatrix},$$

where the units are the same as before.

Finally, the following quantifies the repeatability of [K] (in terms of its 3x3 sub-matrices) by listing the average differences between all empirically determined [K]s. The first measure quantifies repeatability for [K]s measured while the robot remained in one of the two configurations. The second measure quantifies repeatability for [K]s measured while the robot was in either of the two configurations.

3x3 Sub-Matrix[4]	First Measure	Second Measure
upper-left	1%	8%
lower-left	1%	8%
upper-right	5%	13%
lower-right	4%	7%

3 Implementation of 6 DOC Wrench Control

Six degree-of-constraint wrench control was implemented on the experimental apparatus illustrated in Figure 1. A desired wrench was commanded to the KINESTATIC computer, which generated a corrective twist ($\hat{D}_C = [\delta\vec{x}_{OC};\ \delta\vec{\phi}_C]$) based on the control law,

$$\hat{D}_C = -G\,[K]^{-1}\,\hat{w}, \qquad (8)$$

where $\hat{w} = [f_x, f_y, f_z; m_x, m_y, m_z]^T$ expressed in **F** is the difference between the desired and actual wrenches. (The scalar gain G was 0.03.) Eq. (8) was performed approximately every 100 milliseconds, and each time it generated a new twist command.

Before commanding $\hat{D}_C$, it was necessary to first transform it into $\hat{D} = [\delta\vec{x}_O;\ \delta\vec{\phi}]$, where

$$\delta\vec{x}_O = [R_3]\,\delta\vec{x}_{OC} \quad \text{and} \quad \delta\vec{\phi} = [R_3]\,\delta\vec{\phi}_C, \qquad (9)$$

[4]The values given for the upper-left 3x3 matrix are valid for elements in the 3 – 12 kg/cm range. The values given for the lower-left and upper-right 3x3 matrices are valid for elements with a magnitude in the 25 – 40 kg range, and the values given for the lower-right 3x3 matrix are valid for elements in the 75 – 400 kg-cm range.

and where $[R_3]$ is a 3x3 rotation matrix. The columns of $[R_3]$ are the direction cosines of the coordinate axes of **F** expressed in terms of a coordinate system **G**. The origins of **F** and **G** are the same, but the coordinate axes of **G** are parallel to those of the grounded system located at the shoulder of the GE Robot. (The coordinate system at the shoulder of the robot is labeled as **R**.)

The result of (9) was communicated to the ROBOT computer, which controlled the position and orientation of the end-effector (force/torque sensor). The ROBOT computer performed its reverse and forward displacement kinematics every 20 milliseconds, and each time it communicated the results of the forward displacement analysis to the KINESTATIC computer. Figure 3 illustrates the response to a step input of $\hat{w}_i = [0, -1 \text{ kg}, 4 \text{ kg}; 3 \text{ kg-cm}, 2 \text{ kg-cm}, 1 \text{ kg-cm}]^T$, given in terms of **F**.

It is interesting to examine the response shown in Figure 3. This was a typical response – the largest errors being in m_x and m_y. This is because these coordinates measured torques in the x and y directions that, taken together with their corresponding twists, constituted the stiffest twist-wrench combinations. (The coordinates of these twists are respectively the fourth and fifth columns of $[K]^{-1}$.) Consequently, small errors in these twists were magnified as shown in Figure 3.

The investigator realized that placing bounds on these coordinates was necessary. For instance, -8 kg-cm$<m_x<8$ kg-cm, -2 kg$<f_x<2$ kg, and -5 kg$<f_z<5$ kg. This was necessary because the [K] measured in Section 2 and used in (8) was no longer accurate when the compliant device was under loads outside of these bounds. (These bounds also affected where a controlled force could be located. For example, a 1 kg force in the z-direction could not be accurately controlled if it had more than an 8 cm moment about the x-axis.)

A further examination of Figure 3 indicates that the lags were the same for all coordinates. (This was typical in the response plots of other, different wrench step changes.) It is important to recognize this, because this proves the principle that at each instant the wrench error is nulled by the best corrective twist. In other words, the wrench error coordinates are nulled at the same pace.

4 Implementation of 5DOC/1DOF Kinestatic Control

Five degree-of-constraint/one degree-of-freedom kinestatic control was implemented on the experimental apparatus illustrated in Figure 4. The gripper was bolted to a slider (prismatic) joint that was in turn bolted to the level table. Relative to the slider, the gripper was positioned and oriented in a general way.

The twist of freedom of the gripper was $\hat{D}_b = [-1, 0, 0; 0, 0, 0]^T$, which was a translation in the negative x-direction of **G**. (It was also a translation in the negative x-direction of **R**, the grounded coordinate system located at the shoulder of the robot). The position of the slider was p, where $0<p<8$ cm. Figure 4 clearly illustrates that the compliant device was *not* positioned in a general way relative to the slider, and consequently, the experiments demonstrated the general control of this type of gripper constraint.

Because of the bounds placed on controllable wrenches (See Section 3.), judicious choices had to be made regarding which wrenches of constraint to control. Three (m_1, m_2, and m_3) of the five constraints were torques whose directions were those specified by the coordinate axes of **F**. The other two constraints (f_1 and f_2) were forces along respectively the y and z axes of **G**. A desired wrench of constraint was conveniently expressed in terms of **F** by

$$\hat{w}_i = [a]\, \underline{f}_i, \tag{10}$$

where the columns of the 6x5 matrix [a] were the coordinates (in terms of **F**) of the five constraint wrenches, and where $\underline{f}_i = [f_1, f_2, m_1, m_2, m_3]^T$.

While the five columns of [a] were the coordinates of the wrenches of constraints expressed in terms of **F**, it was necessary to declare a sixth wrench that was independent of the wrenches of constraint. This was because the force/torque sensor reported a general wrench ($\hat{w}_s$ in terms of **F**), and it was necessary to filter it into an actual wrench of constraint ($\hat{w}_o$ in terms of **F**). Accordingly, a sixth wrench was declared whose coordinates constituted first column of the 6x6 matrix [m], and

$$[m] = \begin{bmatrix} [R_3]^T & [0_3] \\ [0_3] & [1_3] \end{bmatrix}, \tag{11}$$

where the last five columns correspond to the five columns of [a]. The 3x3 sub-matrix $[R_3]$ was defined in (9), $[0_3]$ is a 3x3 zero matrix, and $[1_3]$ is a 3x3 identity matrix. The filtering of the sensed wrench was then accomplished by the relation,

$$\hat{w}_o = [m][i][m]^{-1}\, \hat{w}_s, \tag{12}$$

wnere [i] is a 6x6 identity matrix whose first element is replaced by a zero, and where $[m]^{-1} = [m]^T$. There were no working wrenches (the friction of the slider was considered minimal), and the assumption was made that the actual wrench of constraint ($\hat{w}_o$) was insensitive to which sixth wrench was chosen to be the first column of [m]. In other words, the first element of $[m]^T\, \hat{w}_s$ is small.

A desired set of five constraints (f_1, f_2, m_1, m_2, and m_3) together with a desired position (p) of the slider was commanded to the KINESTATIC computer, which generated a corrective twist ($\hat{D} = [\delta\vec{x}_o; \delta\vec{\phi}]$) based on the control law:

$$\hat{D} = G_1 \delta p\, \hat{D}_b + G_2\, \hat{D}_c, \tag{13}$$

where $\hat{D}_c$ is the coordinates of the twist of compliance expressed in **G**, where δp is an error in slider position, and where the twist and wrench gains are G_1 and G_2. The coordinates $\hat{D}'_c$ of the twist of compliance expressed in **F** was calculated from

$$\hat{D}'_c = -[K]^{-1}\, (\hat{w}_i - \hat{w}_o), \tag{14}$$

where $\hat{w}_i$ is from (10) and $\hat{w}_o$ is from (12). The coordinates $\hat{D}'_c$ were transformed into $\hat{D}_c$ by (9) where $\hat{D}_c$ is replaced by $\hat{D}'_c$ and where D is replaced by $\hat{D}_c$. Equation (13) was calculated approximately every 100 milliseconds, and the result was communicated to the ROBOT computer.

Representative response plots of this system are given in Figures 5 – 7. Figure 5 illustrates the nulling of a wrench of constraint for initially loaded gripper. It is important to recognize that for this experiment, the twist gain was set to zero, $G_1 = 0$. ($G_2 = 0.03$.) This further illustrates that the twist of compliance used to null the wrench of constraint error was the best twist, since it did not move the slider significantly while nulling a wrench of constraint. (Figure 5 shows constraint response curves with the same type of lagging that was present in the 6 DOC wrench control, and also, it shows that the displacement of the slider was only minimal with some drift.)

Figure 6 illustrates the response of the system that was given a displacement command $p = 5$ cm, and a constraint command, $f_1 = f_2 = m_1 = m_2 = m_3 = 0.0$. The system accomplished the move in 40 seconds, and the constraint forces and torques were suppressed throughout the move. ($G_1 = 0.008$)

Figure 7 illustrates the response of the system that was initially given a step command of $p = 4.0$, $f_1 = 0.$, $f_2 = -1$

kg, $m_1 = 4$ kg-cm, $m_2 = -5$ kg-cm, $m_3 = 2$ kg-cm. Midway through the response, the displacement command was changed to $p = 7.0$ cm. The constraint response curves continued to exhibit lags that were similar, which is indicative of the fact that the correct twist of compliance was commanded at every instant.

Acknowledgement

The authors acknowledge the support of the National Science Foundation, Grant No. MSM – 8810017.

References

[1] Griffis, M., and Duffy, J., 1990, "Kinestatic Control: A Novel Theory for Simultaneously Regulating Force and Displacement," Proc. 21st ASME Mechanisms Conference, Chicago.

[2] Whitney, D., 1982, "Quasi-Static Assembly of Compliantly Supported Rigid Parts," ASME Journal of Dynamic Systems, Measurement, and Control, Vol 104.

[3] Roberts, R., Paul, R., and Hillberry, B., 1985, "The Effect of Wrist Force Sensor Stiffness on the Control of Robot Manipulators," Proc. IEEE International Conference on Robotics and Automation, St Louis, MO.

[4] Xu, Y., and Paul, R., 1988, "On Position Compensation and Force Control Stability of a Robot with a Compliant Wrist," Proc. IEEE International Conference on Robotics and Automation, Philadelphia, PA.

[5] Goswami, A., Peshkin, M., and Colgate, E., 1990, "Passive Robotics: An Exploration of Mechanical Computation," Proc. IEEE International Conference on Robotics and Automation, Cincinnati, OH.

[6] Hennessey, M., 1986, "Robotic Force Tracking Using an IRCC," Proc. of the Winter ASME Annual Meeting, Anahiem CA, DSC-Vol. 3.

[7] Griffis, M., 1991, "Kinestatic Control: A Novel Theory for Simultaneously Regulating Force and Displacement," Ph. D. Dissertation, University of Florida.

[8] Ryan, P., 1986, *Euclidean and Non-Euclidean Geometry: An Analytic Approach*, Cambridge Unversity Press, Cambridge, Eng.

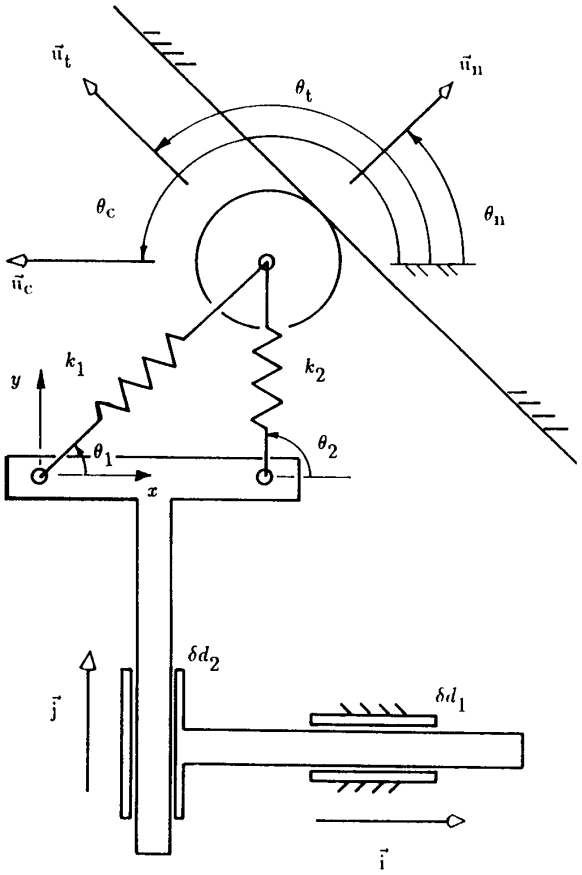

Figure 2.

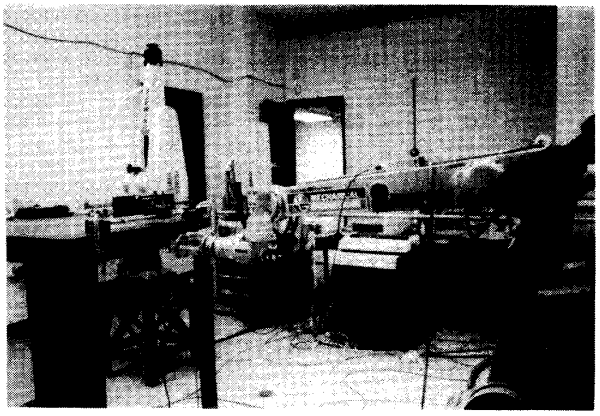

Figure 1.

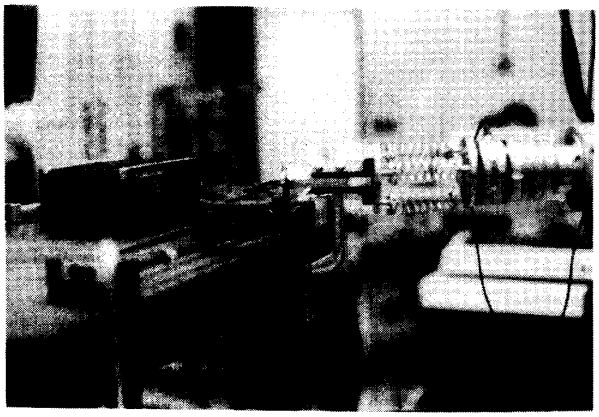

Figure 4.

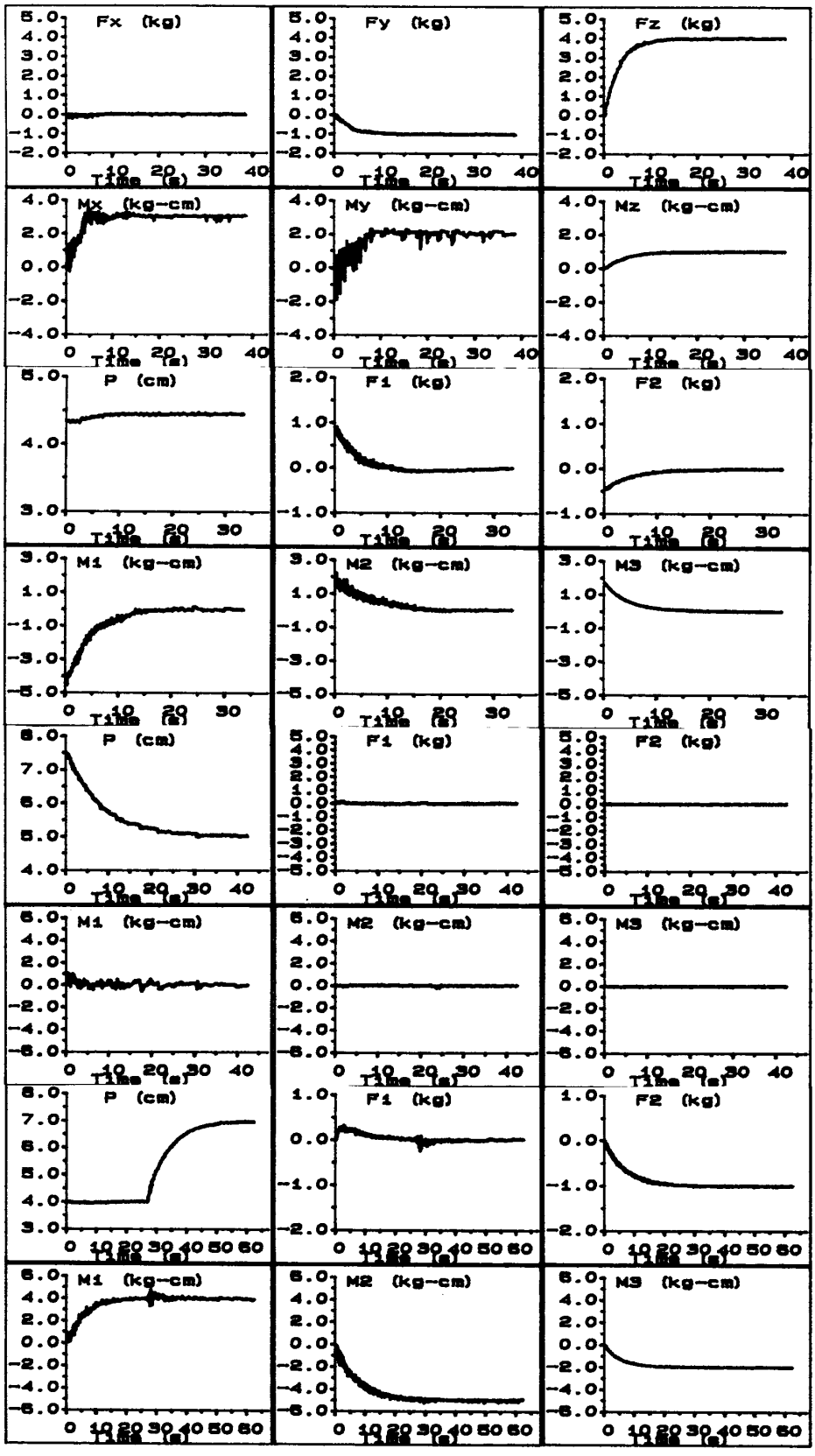

Figure 3.

Figure 5.

Figure 6.

Figure 7.